Torsional Design of Round HSS Members— A Critical Review

BO DOWSWELL

ABSTRACT

Shear yielding is the controlling limit state for most round HSS members subjected to torsion; however, buckling is a limit state that can reduce the torsional strength of members with high diameter-to-wall thickness (*D*/*t*) ratios. The purposes of this paper are to summarize the available research on the torsional performance of round HSS members and evaluate the applicable provisions in the AISC *Specification*. A historical review of the available research revealed 125 experimental tests from seven projects, leading to evolving design methods over the last century. An evaluation of the AISC *Specification* provisions indicated an appropriate reliability level for the yielding limit state; however, the target reliability for buckling is met only for long specimens. A new equation is proposed to predict the buckling strength of intermediate-length members.

Keywords: round HSS, torsion, *D*/*t* ratio, shear yielding, buckling.

INTRODUCTION

For most round HSS members subjected to torsion, shear yielding is the controlling limit state; however, buckling is a limit state that can reduce the torsional strength of members with high diameter-to-wall thickness, D/t, ratios. Many of the available design equations for the buckling strength of round hollow structural members are based on research related to thin-walled cylindrical shells such as tanks, silos and airplane components. The geometries, fabrication methods, and imperfections for these structures can be dramatically different from those of round HSS members. Also, much of the experimental research used materials such as aluminum, brass, and rubber, which have different material behaviors compared to steel. The purposes of this paper are to summarize the research on the torsional performance of round HSS members and compare the available experimental results to the applicable provisions in the AISC *Specification for Structural Steel Buildings* (2022), hereafter referred to as the AISC *Specification*.

AISC *SPECIFICATION* SECTION H3

The nominal torsional strength of an HSS member is calculated using Equation H3-1 from AISC *Specification* Section H3.1.

$$T_n = F_{cr}C \qquad \text{(H3-1)}$$

The available torsional strength is $\phi_T T_n$ (LRFD) or T_n/Ω_T (ASD), as applicable. For round HSS members, the critical shear stress is the largest value from Equations H3-2a and H3-2b but not exceeding the shear yield stress, $0.6F_y$.

$$F_{cr} = \frac{1.23E}{\sqrt{\dfrac{L}{D}} \left(\dfrac{D}{t}\right)^{5/4}} \qquad \text{(H3-2a)}$$

$$F_{cr} = \frac{0.60E}{\left(\dfrac{D}{t}\right)^{3/2}} \qquad \text{(H3-2b)}$$

where

C = torsional constant, in.^{3}
D = outside diameter, in.
L = member length, in.
t = design wall thickness, in.
ϕ_T = 0.90 (LRFD)
Ω_T = 1.67 (ASD)

SECTION PROPERTIES

The polar moment of inertia of a round cross section is (Holland, 1970; Seaburg and Carter, 1997)

$$J = \frac{\pi}{2}\left(R^4 - R_i^4\right) \qquad \text{(1)}$$

$$= \frac{\pi}{32}\left(D^4 - D_i^4\right)$$

$$= \frac{\pi}{4}\left(D - t\right)^3 t$$

Bo Dowswell, PhD, PE, Principal, ARC International, LLC, Birmingham, Ala. Email: bo@arcstructural.com

Table 1. Ovalization Tolerances and Imperfection Reduction Factors in Eurocode 3, Part 1-6 (CEN, 2007).					
			ρ_{max}		
Quality Class	**Description**	α_τ	**$D \le 20$ in.**	**20 in. $< D < 49$ in.**	**$D \ge 49$ in.**
Class A	Excellent	0.75	0.014	$0.007 + (49 - D)/4143$	0.007
Class B	High	0.65	0.020	$0.010 + (49 - D)/2900$	0.010
Class C	Normal	0.50	0.030	$0.015 + (49 - D)/1933$	0.015

As discussed in AISC *Specification* Section H3.1 Commentary, the torsional constant can be defined as the polar moment of inertia divided by the radius at the mid-thickness.

$$C = \frac{2J}{D - t} \tag{2}$$

$$= \frac{\pi}{2}(D - t)^2 t$$

$$= \frac{\pi}{2} D_m^2 t$$

where
D_i = inside diameter, in.
D_m = mean diameter, in.
R = outside radius, in.
R_i = inside radius, in.

EUROCODE 3, PART 1-6

The design equations in Eurocode 3, Part 1-6 (CEN, 2007), are applicable to both clamped and pinned end conditions. The effects of both inelastic buckling in the transition zone and geometric imperfections are considered explicitly. The nominal stress is:

$$\tau_n = \chi \tau_y \tag{3}$$

When $\lambda \le \lambda_p$

$$\chi = 1.0 \tag{4}$$

When $\lambda_p < \lambda \le \lambda_r$

$$\chi = 1.0 - 0.6 \frac{\lambda - \lambda_p}{\lambda_r - \lambda_p} \tag{5}$$

When $\lambda > \lambda_r$

$$\chi = \frac{\alpha_\tau}{\lambda^2} \tag{6}$$

Where the shear yield stress is:

$$\tau_y = \frac{F_y}{\sqrt{3}} \tag{7}$$

the nondimensional slenderness is:

$$\lambda = \sqrt{\frac{\tau_y}{\tau_{cr}}} \tag{8}$$

The limiting slenderness parameter for compact elements is:

$$\lambda_p = 0.4 \tag{9}$$

and the limiting slenderness parameter for noncompact elements is:

$$\lambda_r = \sqrt{2.5\alpha_\tau} \tag{10}$$

where the imperfection reduction factor, α_τ, is selected from Table 1 based on the fabrication quality class.

The critical buckling stress is:

$$\tau_{cr} = 0.75 E C_\tau \frac{t}{R\sqrt{\omega}} \tag{11}$$

The dimensionless length parameter is:

$$\omega = \frac{L}{\sqrt{Rt}} \tag{12}$$

For medium-length cylinders, which are defined by $10 \le \omega \le 8.7R/t$,

$$C_\tau = 1.0 \tag{13}$$

For long cylinders, which are defined by $\omega > 8.7R/t$,

$$C_\tau = \frac{1}{3}\sqrt{\omega \frac{t}{R}} \tag{14}$$

HISTORICAL REVIEW

The *Specification* requirements are based on the theoretical equations that were derived for the elastic critical buckling stresses by various researchers. The equations were derived for tubular sections with length-to-diameter ratios that are categorized as short, moderate-length, and long cylinders.

Schwerin (1924)

Schwerin (1924) developed Equation 15 to predict the critical stress of round HSS members in torsion.

$$\tau_{cr} = 0.248E\left(\frac{t}{R}\right)^{3/2}\left(1+0.45\frac{t}{R}\right) \qquad (15)$$

Donnell (1935) showed that Equation 15 is accurate only for longer members and noted that the value in the second parenthesis is approximately unity, resulting in Equation 16.

$$\tau_{cr} = 0.248E\left(\frac{t}{R}\right)^{3/2} \qquad (16)$$

$$= \frac{0.701E}{\left(\frac{D}{t}\right)^{3/2}}$$

Sezawa and Kubo (1931)

Sezawa and Kubo (1931) believed that the equations developed by Schwerin (1924) were incorrect due to "certain misconceptions." Sezawa and Kubo derived theoretical equations for long cylinders, which showed that the end conditions have a negligible influence on the critical buckling stress. The buckled shapes were characterized by two waves that formed a helical curve with a 27.5° angle from the longitudinal axis of the cylinder as shown in Figure 1. With $n = 2$ (two circumferential buckling waves), the load was minimized to determine the critical stress according to Equation 17, which is applicable only when $L/D \geq 2$. For steel, Poisson's ratio, ν, is 0.3.

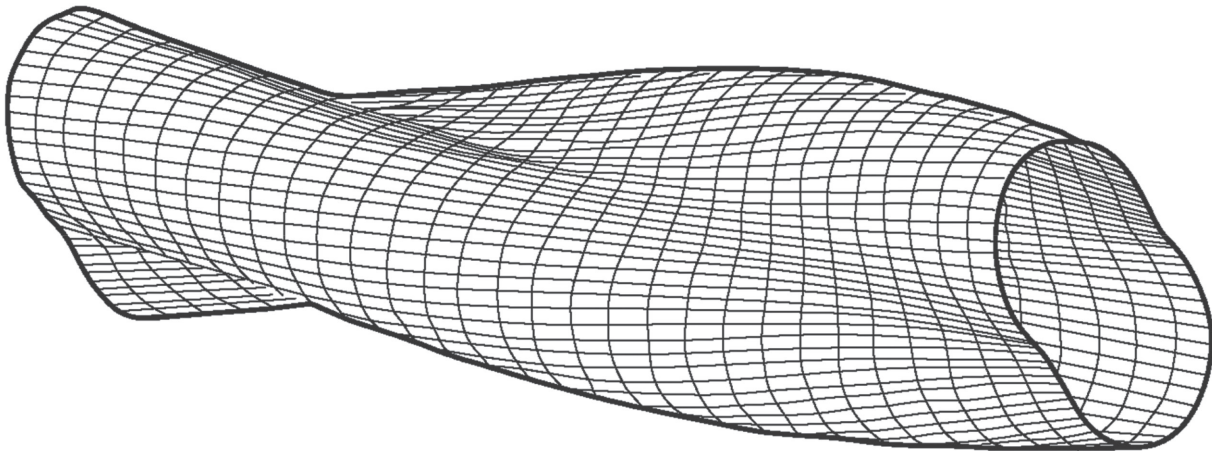$$\tau_{cr} = \frac{0.563E}{1-\nu^2}\left(\frac{t}{R}\right)^2 \qquad (17)$$

$$= \frac{2.47E}{\left(\frac{D}{t}\right)^2}$$

Lunquist (1932)

Based on experimental tests on duralumin cylinders, Lunquist (1932) proposed a critical buckling stress of

$$\tau_{cr} = \frac{k_s E}{\left(\frac{R}{t}\right)^c} \qquad (18)$$

where
   c = constant that was determined empirically to be 1.35
   k_s = coefficient that varies with the L/R ratio

The research showed that the number of buckling waves increases with an increase in the R/t ratio and decreases with increase in the L/R ratio. The specimens in Figure 2 show the effect of the L/R ratio. Small geometric imperfections caused minor buckling distortions below the buckling failure load without significantly affecting the strength. Although the short cylinders had a significant post-buckling strength increase, long cylinders had negative post-buckling strength.

Donnell (1935)

Donnell (1935) derived the differential equations of equilibrium in a simpler form than previous researchers by neglecting several items that would be included in an exact analysis. Many terms in the equilibrium conditions and the term relating the change in curvature to the change in the radius of the buckled shape were neglected. Additionally, the variation in length of the circumferential fibers along the thickness was neglected. For long cylinders where $n = 2$, many studies have shown that Donnell's approximate solution is about 10% higher than that of an exact analysis (Chen, 2016) and the experimental buckling stresses averaged about 75% of those calculated with the proposed

Fig. 1. Buckled shape for n = 2.

design equation. For short and moderately long cylinders with simply supported edges Donnell's theoretical approximation of the critical buckling stress is [7]:

$$\tau_{cr} = \frac{E}{1-\nu^2}\left(\frac{t}{L}\right)^2\left[2.8 + \sqrt{2.6 + 1.40\frac{L^3}{(tD)^{3/2}}(1-\nu^2)^{3/4}}\right]$$

(19)

Substituting $\nu = 0.3$ into Equation 20 and multiplying by 0.6 to get a lower-bound curve results in Donnell's proposed design equation:

$$\tau_{cr} = E\left(\frac{t}{L}\right)^2\left[1.8 + \sqrt{1.2 + 0.57\frac{L^3}{(tD)^{3/2}}}\right]$$

(20)

L/R = 0.87
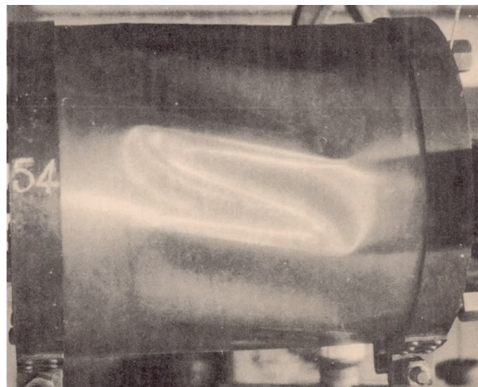
L/R = 2.0

L/R = 3.0

Fig. 2. Buckled specimens from Lundquist (1932).

Batdorf, Schildcrout, and Stein (1947)

According to the theoretical derivation by Batdorf et al. (1947), the elastic critical stress of a thin-walled cylinder loaded in torsion is:

$$\tau_c = k_s \frac{\pi^2 E}{12(1-\nu^2)\left(\dfrac{L}{t}\right)^2} \tag{21}$$

The value for k_s was determined by successive calculations to minimize the critical stress. For simply supported intermediate-length cylinders, k_s is calculated with Equation 22.

$$k_s = 0.85 Z^{3/4} \tag{22}$$

The length ratio, now known as Batdorf's parameter, is:

$$Z = \frac{L^2}{Rt}\sqrt{1-\nu^2} \tag{23}$$

$$= 2\left(\frac{L}{D}\right)^2\left(\frac{D}{t}\right)\sqrt{1-\nu^2}$$

When $\nu = 0.3$, Equation 23 simplifies to:

$$Z = 1.91\left(\frac{L}{D}\right)^2\left(\frac{D}{t}\right) \tag{24}$$

Substituting Equations 22 and 23 into Equation 21 results in Equation 25.

$$\tau_c = \frac{0.85\pi^2 E}{12(1-\nu^2)^{5/8}}\left(\frac{t}{R}\right)^{5/4}\sqrt{\frac{R}{L}} \tag{25}$$

$$= \frac{1.43\pi^2 E}{12(1-\nu^2)^{5/8}}\left(\frac{t}{D}\right)^{5/4}\sqrt{\frac{D}{L}}$$

When $\nu = 0.3$, Equation 25 simplifies to:

$$F_{cr} = \frac{1.25 E}{\sqrt{\dfrac{L}{D}}\left(\dfrac{D}{t}\right)^{5/4}} \tag{26}$$

For long cylinders, the buckled configuration was the same as that described by Sezawa and Kubo (1931), where two circumferential waves formed a helical curve along the cylinder. The critical stress of long cylinders, which was found to be dependent on the R/t ratio, deviated from that of short cylinders at approximately $Z = 10(R/t)^2$. Due to simplifications in the derivation based on the assumption that n^2 is much greater than 1, Batdorf et al. (1947) noted that Equation 26 may be accurate only in the approximate range, $100 \leq Z \leq 10(R/t)^2$.

Sturm (1948)

Sturm (1948) simplified a theoretical solution for graphical representation according to Equation 27. Coefficient K_D is plotted against the L/D ratio in Figure 3. The family of curves, which are based on the D/t ratio, show that the number of buckling waves (labeled N in Figure 3) is dependent on both the L/D and D/t ratio. However, for practical geometries of HSS members used in steel structures, the buckled shape is characterized by only two waves.

$$\tau_{cr} = \frac{K_D E}{\left(\dfrac{D}{t}\right)^2} \tag{27}$$

where

K_D = coefficient that varies with the L/D and D/t ratios

Sturm (1948) also derived a theoretical solution for the circumferential stress caused by initial geometric imperfections, which were assumed to be identical to the buckled shape. For typical round HSS member geometries, the geometric imperfections caused only a 6% stress increase compared to a perfectly round section.

Timoshenko and Gere (1961) and Flugge (1973)

Timoshenko and Gere (1961) and Flugge (1973) developed Equation 28 for the elastic shear buckling stress of infinitely long cylinders by solving the differential equations of equilibrium of the buckled shape.

$$\tau_{cr} = \frac{E}{3\sqrt{2}(1-\nu^2)^{3/4}}\left(\frac{t}{R}\right)^{3/2} \tag{28}$$

When $\nu = 0.3$, Equation 28 simplifies to:

$$\tau_{cr} = \frac{0.716 E}{\left(\dfrac{D}{t}\right)^{3/2}} \tag{29}$$

Gerard (1962) and Schilling (1965)

Based on the experimental results summarized by Batdorf et al. (1947), Gerard (1962) recommended a reduction factor of 0.85 to account for the lower strength caused by imperfections in intermediate-length shells. Schilling (1965) applied this reduction to Equation 26, resulting in Equation 30.

$$\tau_c = \frac{1.06 E}{\sqrt{\dfrac{L}{D}}\left(\dfrac{D}{t}\right)^{5/4}} \tag{30}$$

By setting Equation 30 equal to the shear yield stress, τ_y, Schilling (1965) determined the transition point between

buckling and yielding. He noted that the shear yielding limit state is applicable when

$$\frac{\tau_y}{E}\sqrt{\frac{L}{D}}\left(\frac{D}{t}\right)^{5/4} \leq 1.06 \qquad (31)$$

and shear buckling is applicable when

$$\frac{\tau_y}{E}\sqrt{\frac{L}{D}}\left(\frac{D}{t}\right)^{5/4} > 1.06 \qquad (32)$$

Sherman (1975)

Sherman (1975) recommended using Equations H3-2a and H3-2b for hot-formed intermediate-length and long members, respectively. Due to the rounded stress-strain curves for cold-formed members, equations defining an inelastic

transition region were developed. The equations were based on recommendations by Felton and Dobbs (1967) for aluminum members. For intermediate-length members, elastic buckling is defined by the range

$$\frac{D}{t} > \frac{3.09}{\left(\dfrac{L}{D}\right)^{2/5}}\left(\frac{E}{F_y}\right)^{4/5} \qquad (33)$$

The elastic critical buckling stress is calculated with Equation H3-2a. The inelastic transition zone is defined by the range

$$0.530\left(\frac{E}{F_y}\right)^{2/3} < \frac{D}{t} \leq \frac{3.09}{\left(\dfrac{L}{D}\right)^{2/5}}\left(\frac{E}{F_y}\right)^{4/5} \qquad (34)$$
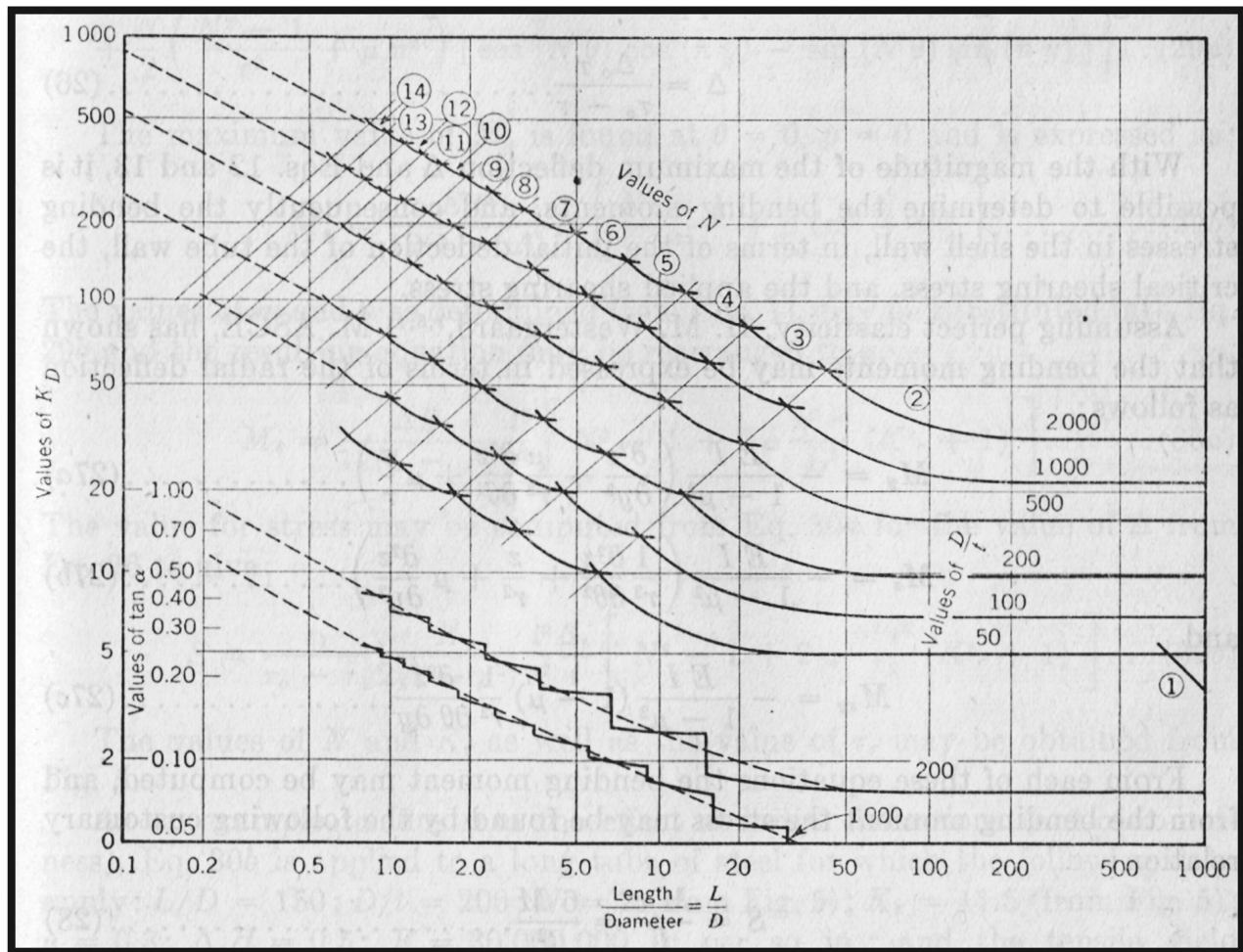

Fig. 3. K_D versus L/D for various D/t ratios (Sturm, 1948).

The inelastic buckling stress in the transition zone is:

$$\tau_c = \tau_y \left[\frac{1 - 0.363\left(\dfrac{L}{D}\right)^{2/5}}{1 - 0.0727\left(\dfrac{L}{D}\right)^{2/5}}\right]\left[1 + \frac{1.89}{\left(\dfrac{E}{F_y}\right)^{2/3}}\left(\frac{D}{t}\right)\right] \quad (35)$$

The limit state is shear yielding when

$$\frac{D}{t} \le 0.530\left(\frac{E}{F_y}\right)^{2/3} \quad (36)$$

For long members, elastic buckling is defined by the range

$$\frac{D}{t} > 1.59\left(\frac{E}{F_y}\right)^{2/3} \quad (37)$$

The elastic critical buckling stress is calculated with Equation H3-2b. The inelastic transition zone is defined by the range

$$0.530\left(\frac{E}{F_y}\right)^{2/3} < \frac{D}{t} \le 1.59\left(\frac{E}{F_y}\right)^{2/3} \quad (38)$$

The inelastic buckling stress in the transition zone is:

$$\tau_c = \tau_y \left[1 - \frac{0.378}{\left(\dfrac{E}{F_y}\right)^{2/3}}\left(\frac{D}{t}\right)\right] \quad (39)$$

The limit state is shear yielding when

$$\frac{D}{t} \le 0.530\left(\frac{E}{F_y}\right)^{2/3} \quad (40)$$

Ellinas, Supple, and Walker (1984)

For elastic buckling, Ellinas et al. (1984) recommended Equation 30 for intermediate-length cylindrical members, which have length-to-diameter ratios in the range

$$\frac{5.12}{\sqrt{\dfrac{D}{t}}} \le \frac{L}{D} \le 1.09\sqrt{\frac{D}{t}} \quad (41)$$

Equation 42, which was developed by multiplying Equation 29 by a reduction factor of 0.73 to account for imperfections, was recommended for long cylinders.

$$\tau_{cr} = \frac{0.524E}{\left(\dfrac{D}{t}\right)^{3/2}} \quad (42)$$

where long cylinders are defined by the range

$$\frac{L}{D} > 1.09\sqrt{\frac{D}{t}} \quad (43)$$

To account for inelastic effects in long cylinders, a torsional parameter, α_t, was introduced.

$$\alpha_t = \frac{E}{\tau_y}\left(\frac{t}{D}\right)^{3/2} \quad (44)$$

For elastic buckling, which is defined by the range $\alpha_t \le 1.5$, Equation 42 was rewritten as

$$\tau_{cr} = 0.524\alpha_t\tau_y \quad (45)$$

The inelastic transition zone is defined by the range $1.5 < \alpha < 9$ and the buckling stress is:

$$\tau_{cr} = \tau_y\left(0.813 + 0.068\sqrt{\alpha_t - 1.5}\right) \quad (46)$$

when $\alpha > 9$, the limit state is shear yielding.

Zhang and Han (2007)

Based on a theoretical analysis, Zhang and Han (2007) showed that the number of buckling waves and the post-buckling strength decreases with increasing values of Z (and increasing length, L). A sensitivity analysis, which used an initial imperfection shape that was identical to the buckled shape, showed that even small imperfections reduce the buckling load, and the imperfection direction (inward or outward) has no effect on the reduction. The buckling reduction factor, α, is plotted against the normalized imperfection ratio, δ_o/t, in Figure 4.

Devi and Singh (2021)

A parametric study by Devi and Singh (2021) was based on finite element models of steel HSS members with a yield stress of 56.1 ksi. For the nonslender members that failed by shear yielding, the maximum torsional moments from the finite element models were accurately predicted using AISC *Specification* Equation H3-1 with $F_{cr} = 0.6F_y$. However, the strengths were overpredicted by AISC *Specification* Equations H3-1 and H3-2 for the slender sections that failed by buckling. In this case, the mean model-to-calculated ratio was only 0.91.

DISCUSSION

General Comments

Low values of Batdorf's parameter, Z, which is defined according to Equation 23, are typical of short shell structures such as tanks and silos. Almost all HSS structural

members will be either long or intermediate length, with $Z > 2{,}000$.

Definition of Intermediate Length

According to Batdorf et al. (1947), Equation 22, which was developed for intermediate-length cylinders, is applicable in the approximate range, $100 \leq Z \leq 10(R/t)^2$. Gerard (1962) recommended a range of applicability of $50 \leq Z \leq 10(1 - v^2)(R/t)^2$, Schilling (1965) recommended a range of $50 \leq Z \leq 9(R/t)^2$, and Ziemian (2010) recommended $100 \leq Z \leq 19.2(1 - v^2)(D/t)^2$. The range defined by NASA (1965) was adjusted to include an imperfection factor, resulting in $50 \leq 0.59Z \leq 78(1 - v^2)(R/t)^2$. Gerard's range is equivalent to:

$$\frac{5.12}{\sqrt{\dfrac{D}{t}}} \leq \frac{L}{D} \leq 1.09\sqrt{\frac{D}{t}} \qquad (47)$$

The range defined in Ziemian (2010) is equivalent to

$$\frac{7.24}{\sqrt{\dfrac{D}{t}}} \leq \frac{L}{D} \leq 3.03\sqrt{\frac{D}{t}} \qquad (48)$$

The range defined by Eurocode 3, Part 1-6 (CEN, 2007), $10 \leq \omega \leq 8.7R/t$, is equivalent to

$$\frac{7.07}{\sqrt{\dfrac{D}{t}}} \leq \frac{L}{D} \leq 3.08\sqrt{\frac{D}{t}} \qquad (49)$$

The range defined by NASA (1965) is equivalent to:

$$\frac{6.66}{\sqrt{\dfrac{D}{t}}} \leq \frac{L}{D} \leq 3.97\sqrt{\frac{D}{t}} \qquad (50)$$

AISC *Specification*

AISC *Specification* Equation H3-2a is for intermediate-length members. Intermediate-length members are defined by

$$\frac{L}{D} \leq 4.20\sqrt{\frac{D}{t}} \qquad (51)$$

AISC *Specification* Equation H3-2b was developed using Equation 28, which is for infinitely long cylinders. According to AISC *Specification* Section H3.1 Commentary, the theoretical value for the constant is 0.73; however, this is based on $v = \frac{1}{3}$. Equation 29 shows that the theoretical constant should be 0.716 for $v = 0.3$. Long members are defined by

$$\frac{L}{D} > 4.20\sqrt{\frac{D}{t}} \qquad (52)$$

Because the critical shear stress is defined as the largest value from Equations H3-2a and H3-2b, with a maximum value of $0.6F_y$, the applicability range for each equation is defined by the crossover point where the two equations are equal. Therefore, Equations 51 and 52 are not required for design. In Figure 5, F_{cr} versus L/D is plotted using Equations H3-2a and H3-2b. The curves for $D/t = 50$, 75, and 100
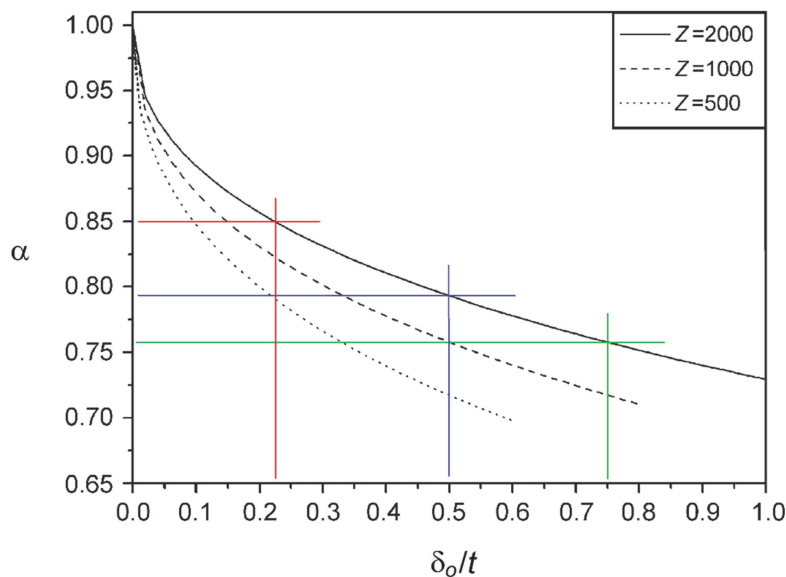
Fig. 4. Buckling reduction factor, α, versus the normalized imperfection ratio, δ_o/t (adapted from Zhang and Han, 2007).

are shown in green, blue, and red, respectively. The horizontal lines represent Equation H3-2b and the curved lines represent Equation H3-2a. The maximum of the two curves for each D/t ratio is shown with the solid lines. The graphs show that intermediate-length members can have significantly more strength than long members.

Cross-Sectional Tolerances

The initial out-of-roundness was defined by Chen and Sohal (1988) with Equation 53, which results in the ovalized shape shown in Figure 6.

$$\delta = \delta_o \cos 2\theta \qquad (53)$$

where
  θ = angle from the major axis of the ovalized shape
  δ_o = maximum initial radial deviation from the nominal shape

δ_o can be defined with Equation 54 using the maximum and minimum diameters of the ovalized shape.

$$\delta_o = \frac{D_{max} - D}{2} \qquad (54)$$
$$= \frac{D - D_{min}}{2}$$

where
  D_{max} = major axis dimension of the ovalized shape
  D_{min} = minor axis dimension of the ovalized shape

In their research, Chen and Sohal (1988) used an ovalization parameter, ρ, of 1%, where the ovalization parameter is:

$$\rho = \frac{D_{max} - D_{min}}{D} \qquad (55)$$
$$= \frac{4\delta_o}{D}$$

Fig. 5. Graph of AISC Specification *Equations H3-2.*

Fig. 6. Ovalization distortion.

This results in $\delta_o = D/400$. Based on the applicable ASTM tolerances, this value is significantly lower than the maximum deviations allowed for these members:

- For 2.00 in. diameter and larger ASTM A500/A500M (2021) and A1085/A1085M (2015a) HSS shapes, the outside diameter does not vary more than ±0.75%, rounded to the nearest 0.005 in., from the specified outside diameter. This results in a maximum δ_o for symmetrical ovalization of $D/267$.

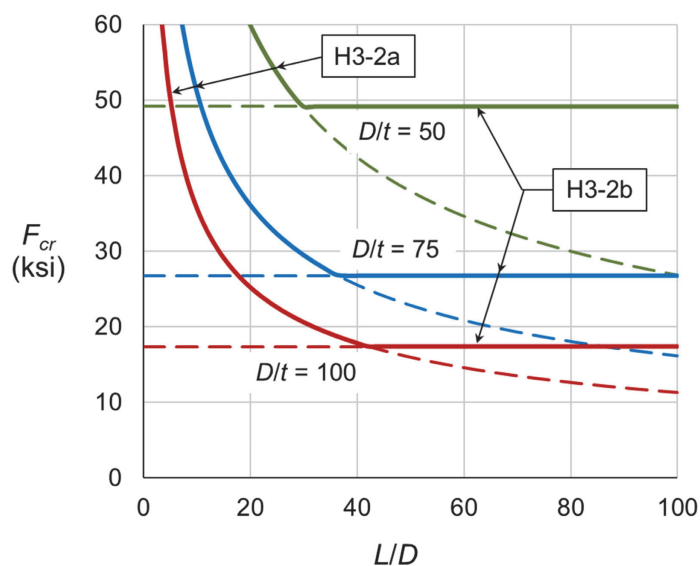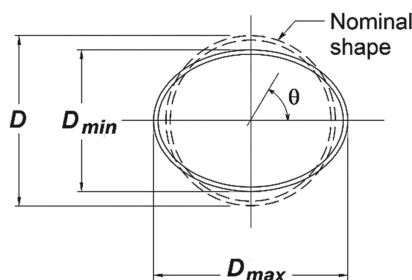- For 2.00 in. diameter and larger ASTM A53/A53M (2020), A501/A501M (2014), and A618/A618M (2015b) HSS shapes, the outside diameter does not vary more than ±1% from the specified outside diameter. This results in a maximum δ_o for symmetrical ovalization of $D/200$.

Table 1 lists the ovalization tolerances, ρ_{max}, specified in Eurocode 3, Part 1-6 (CEN, 2007), based on the fabrication quality class. Class C ovality tolerance is the most reasonable representation of the ASTM pipe and HSS diameter tolerances.

Effect of Imperfections

Nash (1957) showed that the buckling strength of intermediate-length cylinders subjected to torsion is reduced by geometric imperfections. For long cylinders, the buckling mode with $n = 2$ described by Sezawa and Kubo (1931), Batdorf et al. (1947), Sturm (1948), and Schmidt and Wintersetter (2004) is as a helical ovalization of the cross section as shown in Figure 1. For this case, the buckled cross-sectional shape is similar to the initial out-of-roundness imperfection in Figure 6. However, for the current manufacturing methods for HSS members that use linear weld seams, the initial imperfection is expected to be at a constant rotational location along the length instead of forming a helical curve. Although the use of spiral welding is increasing, it is primarily used for shapes with larger diameters.

Loo (1955) used large-deflection theory to determine the effect of initial geometric imperfections on the buckling of cylindrical shells subjected to torsion. For the condition with no geometric imperfection, the results were in close agreement with those of Donnell (1935), which were based on small-deflection theory. The pattern of the initial geometric imperfection was assumed to correspond to the buckled shape. The buckling reduction factor, α, defined by Equation 56, was developed using trial-and-error to best represent the theoretical reductions in buckling stress over a wide range of geometries. The dimensionless length parameter, ω, is defined according to Equation 12.

$$\alpha = 1 - \frac{3}{4}\left(\frac{2\delta_o/t}{\omega^{0.6}}\right)^{0.6} \tag{56}$$

Seide et al. (1960) noted that the experimental buckling loads can be as much as 40% lower than the theoretical small-deflection solutions. The average experimental-to-calculated ratio was 0.84, and the authors recommended a "design" reduction factor of 0.75 for intermediate-length cylinders.

Based on the work of Batdorf et al. (1947) and Timoshenko and Gere (1961), NASA (1965) published reduction factors "to approximate the lower limit of most data." It was determined that the appropriate reduction factors for Equations 26 and 29 are 0.67 and 0.59, respectively.

Imperfections were considered in AISC *Specification* Equation H3-2b by reducing the constant from 0.73 (or 0.716) to 0.60, resulting in a reduction factor of 0.82 (or 0.84). According to AISC *Specification* Section H3.1 Commentary, Equation H3-2a includes a 15% reduction to account for initial imperfections. However, it appears that the 0.85 constant in Equation 22 was erroneously assumed to be a reduction for imperfections. The 0.85 constant was calculated theoretically, and the resulting Equation 26 is different from Equation H3-2a only because $\nu = \frac{1}{3}$ was used in Equation H3-2a instead of $\nu = 0.30$. Batdorf et al. (1947) showed that Equations 26 and H3-2a provide a reasonable upper-bound solution compared to the experimental results that were available at the time. Accordingly, Schilling (1965) recommended that the theoretical critical stress should be reduced by 15%, resulting in a coefficient of $0.85 \times 1.25 = 1.06$, as provided in Equation 30.

For the shapes listed in the 16th Edition *Steel Construction Manual* (AISC, 2023), the highest D/t ratio is 74.5 for a pipe section with $D = 26.0$ in. and $t = 0.349$ in. For this shape the ASTM A53/A53M tolerance is $\delta_o = D/200$, resulting in a maximum permissible $\delta_o/t = 74.5/200 = 0.373$. With a reasonable lower-bound length of 97.5 in., $Z = 2,000$. From Figure 4 with $Z = 2,000$, the buckling reduction factor, $\alpha = 0.85$ at $\delta_o/t = 0.22$ and $\alpha = 0.82$ at $\delta_o/t = 0.373$. Equation 56 results in similar values, with $\alpha = 0.88$ at $\delta_o/t = 0.22$ and $\alpha = 0.84$ at $\delta_o/t = 0.373$.

Post-Buckling Strength

As noted previously by Lunquist (1932), although short cylinders had a significant post-buckling strength increase, long cylinders have negative post-buckling strength. This conclusion was verified by Budiansky (1969), Yamaki (1974), and Zhang and Han (2007).

EXPERIMENTAL COMPARISONS

A review of the available research on the torsional strength of round hollow steel cylinders revealed 125 experimental tests from seven previously published research projects. A total of 106 of the specimens had an ultimate failure mode of buckling. Many of these specimens buckled in the inelastic

range. The remaining 19 specimens failed by yielding with no post-yield buckling. Several of the researchers tested multiple materials; however, only the steel specimens were included in the database used in this paper. The details of all test specimens are listed in Table A1 of Appendix A, and the experimental results are listed in Table A2.

Popplewell and Coker (1895)

Popplewell and Coker (1895) tested five hollow mild steel shafts with a tensile yield stress of 34.8 ksi. The specimens had very large rotations at failure. Because the torsional strengths at the failure rotations were almost three times the first-yield moments, the strengths used in this paper are the first-yield values. Supplementary tension and double-shear tests were also conducted.

Seely and Putnam (1919)

Seely and Putnam (1919) tested six hollow cylinders that were machined from solid round bars to form the desired inner diameter. The bars had outer diameters of 1.88 and 3.75 in. Soft, mild, and medium steels were tested, with tensile yield points of 28.4 ksi, 33.0 ksi, and 46.8 ksi, respectively. All specimens failed by shear yielding.

Bridget, Jerome, and Vosseller (1934)

Bridget et al. (1934) tested nine round HSS specimens with diameters between 0.625 and 2.875 in. The steel specimens had tensile yield stresses between 36.0 and 57.7 ksi. All specimens failed by buckling.

Donnell (1935)

Donnell (1935) tested 30 steel round HSS members between 1.88 in. and 27.0 in. diameter that were proportioned for buckling well below the elastic shear yielding limit. The specimens were fabricated by rolling thin plates to the appropriate diameter and soldering at the longitudinal seam, which were lapped approximately $\frac{1}{16}$ in. The research showed that small-diameter specimens can be used to accurately predict the behavior of much larger members.

Stang, Ramberg, and Back (1937)

Stang et al. (1937) tested 63 chromium-molybdenum steel round HSS members between $\frac{5}{8}$ and 2.5 in. diameter. The tensile yield stresses varied from 67.7 to 110 ksi. The specimens failed by either elastic "two-lobe" buckling with $n = 2$ or inelastic buckling.

Schmidt and Winterstetter (2004)

Schmidt and Winterstetter (2004) tested four specimens of approximately 8 in. diameter and 24 ksi tensile yield stress. All of the specimens failed by buckling.

Wu, He, Ghafoori, and Zhao (2018)

Wu et al. (2018) tested eight round HSS sections that failed by shear yielding before buckling distortion occurred at large rotation angles. The diameters were 3.50, 4.00, and 4.50 in., and the tensile yield strengths were between 41.2 and 58.0 ksi. Additional tests were conducted on specimens that were reinforced with carbon-fiber reinforced polymer (CFRP) composites.

Discussion

For the 19 specimens that failed by yielding, the maximum experimental torsional moment, T_e, was greater than the calculated torsional yield moment, $T_y = 0.6\sigma_y C$, where σ_y is the measured uniaxial yield stress in tension. The specimens tested by Popplewell and Coker (1895) sustained moments of $2.5T_y$ at large rotations; however, experimental measurements indicated that the proportional limit averaged $0.927T_y$.

For designing according to the AISC *Specification*, the critical stress can be defined by either Equation H3-2a or H3-2b. Therefore, the experimental data is plotted in Figure 7 using the controlling slenderness parameter, λ, which corresponds to the equation resulting in the highest critical stress. For Equation H3-2a, the slenderness parameter is:

$$\lambda = \frac{0.6\sigma_y}{1.23E}\sqrt{\frac{L}{D}}\left(\frac{D}{t}\right)^{5/4} \tag{57}$$

For Equation H3-2b, the slenderness parameter is:

$$\lambda = \frac{0.6\sigma_y}{0.60E}\left(\frac{D}{t}\right)^{3/2} \tag{58}$$

Figure 7 shows the AISC *Specification* nominal strength (without ϕ) curve for T_e/T_y versus λ. The LRFD available strength (including ϕ) curve is shown with the dashed line. For the calculation of λ and T_y for the experimental data points, the measured dimensions and material properties were used in lieu of the nominal values. The AISC curve predicts the data trend accurately; however, for λ greater than about 1.5, most of the data points are below the nominal curve and several are well below the LRFD available strength curve.

RELIABILITY ANALYSIS

The resistance factor required to obtain a specific reliability level is (Galambos and Ravinda, 1978):

$$\phi = C_R \rho_R e^{-\beta\alpha_R V_R} \tag{59}$$

where
  C_R = correction factor
  V_R = coefficient of variation

α_R = separation factor

β = reliability index

ρ_R = bias coefficient

Galambos and Ravinda (1973) proposed a separation factor, α_R, of 0.55. For $L/D = 3.0$, Li et al. (2007) developed Equation 60 for calculating the correction factor.

$$C_R = 1.40 - 0.156\beta + 0.0078\beta^2 \qquad (60)$$

Based on AISC *Specification* Section B3.1 Commentary, the target reliability index, β_T, is 2.6, which results in $C_R = 1.05$. The coefficient of variation and bias coefficient are calculated using the statistical parameters of the specific joint. The bias coefficient is:

$$\rho_R = \rho_M \rho_G \rho_P \qquad (61)$$

where

ρ_G = bias coefficient for the geometric properties

ρ_M = bias coefficient for the material properties

ρ_P = bias coefficient for the test-to-predicted strength ratios; mean value of the professional factor calculated with the measured geometric and material properties

The coefficient of variation is:

$$V_R = \sqrt{V_M^2 + V_G^2 + V_P^2} \qquad (62)$$

where

V_G = coefficient of variation for the geometric properties

V_M = coefficient of variation for the material properties

V_P = coefficient of variation for the test-to-predicted strength ratios

The author was unable to locate statistical data regarding deviations from the nominal diameter. However, for members meeting the required ASTM tolerances, any diameter variation results in only a 1% worst-case strength reduction. Historically, the effect of initial imperfections has been addressed with a reduction factor. Therefore, the diameter is considered a deterministic quantity. Also, the effect of length variation was assumed to be negligible. For these conditions, ρ_G and V_G are dependent only on the wall thickness, t.

Osterhof and Driver (2011) used $\rho_t = 1.00$ and $V_t = 0.050$ for the wall thickness characteristics of HSS members. The slightly more conservative values from Dowswell (2021) were used for the calculations in this paper: $\rho_t = 0.994$ and $V_t = 0.050$.

The material characteristics for modulus of elasticity are $\rho_E = 1.04$ and $V_E = 0.026$ (Schmidt and Bartlett, 2002). Liu et al. (2007) determined the material characteristics for yield stress of round HSS members: for A500 Grade B, $\rho_F = 1.36$ and $V_F = 0.07$; for A53 Grade B, $\rho_M = 1.59$, $V_M = 0.11$.
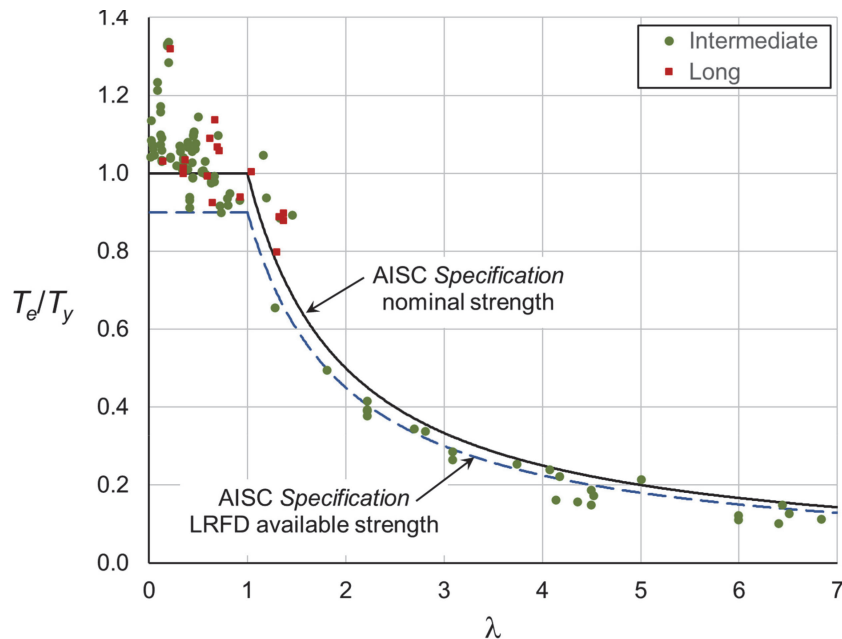

Fig. 7. Graph of AISC Specification *equations with experimental data.*

Table 2. Reliability Functions				
			Buckling	
		Yielding	Intermediate	Long
Material	ρ_M	$\rho_F = 1.36$	$\rho_E = 1.04$	$\rho_E = 1.04$
	V_M	$V_F = 0.07$	$V_E = 0.026$	$V_E = 0.026$
Geometric	ρ_G	$\rho_t = 0.994$	$(\rho_t)^{9/4} = 0.987$	$(\rho_t)^{5/2} = 0.985$
	V_G	$V_t = 0.050$	$(9/4)(V_t) = 0.113$	$(5/2)(V_t) = 0.125$

For the 19 specimens with low wall slenderness parameters, where the maximum value for $(D/t)(F_y/E)$ is 0.0551, the ultimate experimental torsion resulted in large inelastic rotation angles. Therefore, for these specimens, the proportional limit on the torsion-rotation curve was used for the experimental yield torsion.

The reliability analysis must be based on the three equations for yielding, buckling of intermediate-length members, and buckling of long members. For a first-order multivariate analysis, the mean and variance of T_c can be approximated with Equations 63 and 64, respectively (Benjamin and Cornell, 1970).

$$T_{cm} \approx f\left(X_{1m}, X_{2m}, ..., X_{nm}\right) \tag{63}$$

$$\sigma_{T_c}^2 \approx \sum_{i=1}^{n}\left[\left(\frac{\partial T_c}{\partial X_i}\right)_m\right]^2 \sigma_{X_i}^2 \tag{64}$$

where

T_c = critical torsional strength

T_{cm} = mean value of the critical torsional strength

X_i = uncorrelated variables affecting T_c

Substituting Equation 2 into Equation H3-1 and setting F_{cr} equal to $0.6F_y$, the critical torsion for the limit state of yielding is:

$$T_c = 0.3\pi F_y D_m^2 t \tag{65}$$

Because Equation 65 is linear with respect to both F_y and t, the statistical parameters for the geometric and material properties are used without manipulation as listed in the third column of Table 2.

Substituting Equation H3-2a and Equation 2 into Equation H3-1, the buckling strength of intermediate-length members is:

$$T_c = \frac{0.615\pi ED_m^2 t}{\sqrt{\dfrac{L}{D}\left(\dfrac{D}{t}\right)^{5/4}}} \tag{66}$$

Equation 66 is linear with respect to E. The derivative of T_c with respect to t is:

$$\frac{\partial T_c}{\partial t} = \left(\frac{9}{4}\right)\frac{0.615\pi ED_m^2}{\sqrt{\dfrac{L}{D}\left(\dfrac{D}{t}\right)^{5/4}}} \tag{67}$$

The statistical parameters for the geometric and material properties for buckling of intermediate-length members are listed in the fourth column of Table 2. Substituting Equations H3-2b and 2 into Equation H3-1, the buckling strength of long members is:

$$T_c = \frac{0.30\pi ED_m^2 t}{\left(\dfrac{D}{t}\right)^{3/2}} \tag{68}$$

Equation 68 is linear with respect to E. The derivative of T_c with respect to t is:

$$\frac{\partial T_c}{\partial t} = \left(\frac{5}{2}\right)\frac{0.30\pi ED_m^2}{\left(\dfrac{D}{t}\right)^{3/2}} \tag{69}$$

The statistical parameters for the geometric and material properties for buckling of long members are listed in the fifth column of Table 2.

AISC *Specification* Equations

Because the reliability functions are separated into three groups (yielding, buckling of intermediate-length members, and buckling of long members), each group was analyzed separately. Statistical parameters for test-to-predicted strength ratios, ρ_P and V_P, as well as the number of specimens, N, within each group are listed in Table 3.

From Table 3, $\rho_P = 1.00$ when the AISC *Specification* equations are used with all specimens. However, an observation of the statistical parameters for buckling of intermediate-length members reveals the inaccuracy of Equation H3-2a. Using $\phi = 0.90$ resulted in $\beta = 4.06$ for the specimens with a predicted failure mode of yielding, and $\beta = 1.71$ for the intermediate-length specimens with a predicted failure mode of buckling. Because 1.71 is below the target reliability index, Equation 70 is proposed to replace Equation H3-2a.

Table 3. Statistical Parameters for Test-to-Predicted Strength Ratios				Buckling		
		All	**Yielding**	**All**	**Intermediate**	**Long**
AISC Specification	**N**	125	84	41	36	5
	ρ$_P$	1.00	1.02	0.967	0.944	1.14
	V$_P$	0.170	0.112	0.254	0.266	0.0717
Proposed equation	**N**	125	76	49	39	10
	ρ$_P$	1.12	1.02	1.27	1.28	1.23
	V$_P$	0.217	0.115	0.246	0.266	0.187
N = number of specimens						

$$F_{cr} = \frac{0.85E}{\sqrt{\dfrac{L}{D}\left(\dfrac{D}{t}\right)^{5/4}}} \qquad (70)$$

$$\frac{L}{D} \le 2.01\sqrt{\frac{D}{t}} \qquad (71)$$

The statistical parameters for test-to-predicted strength ratios using the proposed equation are listed in Table 3. With $\phi = 0.90$, Equation 70 results in $\beta = 2.64$ for the 39 intermediate-length specimens with a predicted failure mode of buckling. At the target reliability index ($\beta_T = 2.6$), $\phi = 0.910$. The revised range for intermediate-length members is defined by Equation 71.

For the remaining groups, β always exceeded β_T, with the 76 yielding specimens resulting in $\beta = 4.12$ and all 49 buckling specimens resulting in $\beta = 2.98$. Figure 8 shows the proposed nominal strength (without ϕ) curve for T_e/T_y versus λ. The LRFD available strength (including ϕ) curve is shown with the dashed line.
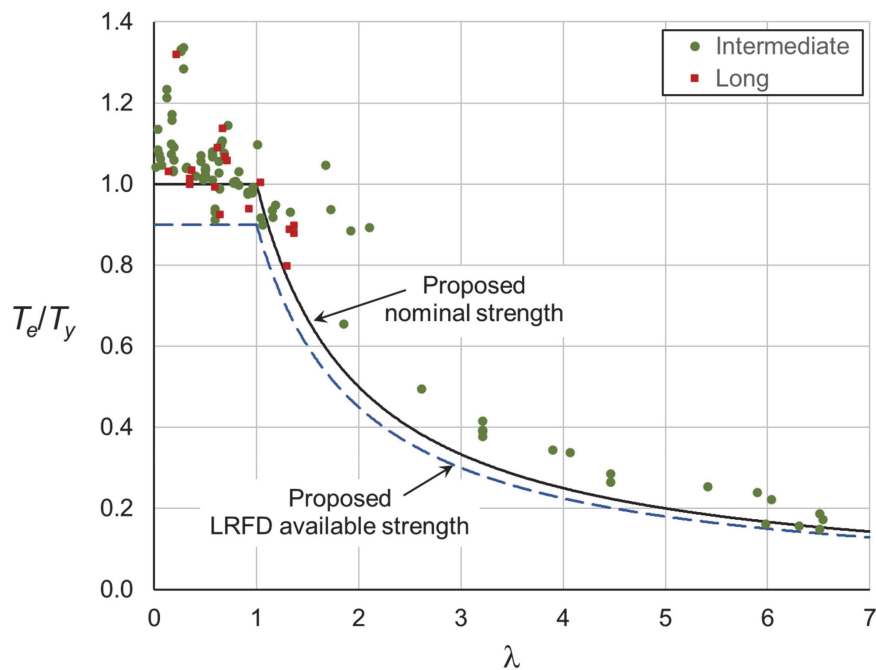

Fig. 8. Graph of proposed equations with experimental data.

CONCLUSIONS

A historical review of the available research on the torsional strength of round HSS members revealed 125 experimental tests from seven projects, leading to evolving design methods over the last century. Theoretical and experimental research indicated two failure modes—yielding and buckling. To consider the effect of length, members with a buckling failure mode were further divided into long and intermediate-length members.

The experimental research showed that members with low wall slenderness parameters, $(D/t)(F_y/E)$, have significant inelastic strength. However, the large inelastic rotation angles required to realize this additional strength make the upper limit, $F_{cr} = 0.6F_y$, for AISC *Specification* H3-1 appropriate based on typical serviceability considerations. Both the theoretical and experimental research indicated that imperfections can significantly reduce the buckling strength.

An evaluation of the AISC *Specification* provisions revealed inconsistent reliability indices that are dependent on the predicted failure mode and the member geometry. The reliability level for the yielding limit state is appropriate; however, the target reliability for buckling is met only for long specimens. For intermediate-length members, the target reliability index can be met if AISC *Specification* Equation H3-2a is replaced with Equation 70.

REFERENCES

AISC (2022), *Specification for Structural Steel Buildings*, ANSI/AISC 360-22, American Institute of Steel Construction, Chicago, Ill.

AISC (2023), *Steel Construction Manual*, 16th Ed., American Institute of Steel Construction, Chicago, Ill.

ASTM (2014), *Standard Specification for Hot-Formed Welded and Seamless Carbon Steel Structural Tubing,* ASTM 501/501M, ASTM International, West Conshohocken, Pa.

ASTM (2015a), *Standard Specification for Cold-Formed Welded Carbon Steel Hollow Structural Sections (HSS),* ASTM 1085/1085M, ASTM International, West Conshohocken, Pa.

ASTM (2015b), *Standard Specification for Hot-Formed Welded and Seamless High-Strength Low-Alloy Structural Tubing,* ASTM 618/618M, ASTM International, West Conshohocken, Pa.

ASTM (2020), *Standard Specification for Pipe, Steel, Black and Hot-Dipped, Zinc-Coated, Welded and Seamless,* ASTM 53/53M, ASTM International, West Conshohocken, Pa.

ASTM (2021), *Standard Specification for Cold-Formed Welded and Seamless Carbon Steel Structural Tubing in Rounds and Shapes,* ASTM 500/500M, ASTM International, West Conshohocken, Pa.

Batdorf, S.B., Schildcrout, M., and Stein, M. (1947), *Critical Stress of Thin-Walled Cylinders in Torsion*, NACA Technical Note No. 1344, July.

Benjamin, J.R. and Cornell, C.A. (1970), *Probability, Statistics and Decision for Civil Engineers*, McGraw-Hill.

Bridget, F.J., Jerome, C.C., and Vosseller, A.B. (1934), "Some New Experiments on Buckling of Thin-Wall Construction," *Transactions of the American Society of Mechanical Engineers*, Applied Mechanics Division, Vol. 56.

Budiansky, B. (1969), "Post-Buckling Behavior of Cylinders in Torsion," *Theory of Thin Shells*, F.I. Niordson, ed., Springer-Verlag.

CEN (2007), *Eurocode 3—Design of Steel Structures—Part 1-6: Strength and Stability of Shell Structures*, Comite Européen de Normalisation, Brussels, Belgium.

Chen, D.H. (2016), *Crush Mechanics of Thin-Walled Tubes*, CRC Press.

Chen, W.F. and Sohal, I.S. (1988), "Cylindrical Members in Offshore Structures," *Thin-Walled Structures*, Vol. 6, pp. 153–285.

Devi, S.V. and Singh, K.D. (2021), "The Continuous Strength Method for Circular Hollow Sections in Torsion," *Engineering Structures*, Vol. 242.

Donnell, L.H. (1935), "Stability of Thin-Walled Tubes under Torsion," *NACA Technical Report No. 479*, National Advisory Committee for Aeronautics.

Dowswell, B. (2021), "Analysis of the Shear Lag Factor for Slotted Rectangular HSS Members," *Engineering Journal*, AISC, Vol. 58, No. 3.

Ellinas, C.P., Supple, W.J., and Walker, A.C. (1984), *Buckling of Offshore Structures—A State-of-the-Art Review*, Gulf Publishing Company.

Felton, L.P. and Dobbs, M.W. (1967), "Optimum Design of Tubes for Bending and Torsion," *Journal of the Structural Division*, ASCE, No. ST 4, August.

Flugge, W. (1973), *Stresses in Shells*, 2nd Ed., Springer-Verlag.

Galambos, T.V. and Ravinda, M.K. (1973), *Tentative Load and Resistance Factor Design Criteria for Steel Buildings*, Research Report No. 18, September, Department of Civil and Environmental Engineering, Washington University, St. Louis, Mo.

Galambos, T.V. and Ravinda, M.K. (1978), "Properties of Steel for Use in LRFD," *Journal of the Structural Division*, ASCE, Vol. 104, No. ST9, September, pp. 1,459–1,468.

Gerard, G. (1962), *Introduction to Structural Stability Theory*, McGraw-Hill.

Holland, M. (1970), *Torsion of Prismatic Members*, Draughtsmen's & Allied Technicians' Association.

Li, C., Grondin, G.Y., and Driver, R.G. (2007), *Reliability Analysis of Concentrically Loaded Fillet Welded Joints*, Structural Engineering Report No. 271, University of Alberta, October.

Liu, J., Sabelli, R., Brockenbrough, R.L., and Fraser, T.P. (2007), "Expected Yield Stress and Tensile Strength Ratios for Determination of Expected Member Capacity in the AISC *Seismic Provisions*," *Engineering Journal*, AISC, Vol. 44, No. 1, pp. 15–25.

Loo, T.T. (1955), "Effects of Large Deflections and Imperfections on the Elastic Buckling of Cylinders under Torsion and Axial Compression," *Proceedings of the Second U.S. National Congress of Applied Mechanics*, American Society of Mechanical Engineers, pp. 345–357.

Lunquist, E.E. (1932), "Strength Tests on Thin-Walled Duralumin Cylinders in Torsion," *NACA Technical Note 427*, National Advisory Committee for Aeronautics.

NASA (1965), *Buckling of Thin-Walled Circular Cylinders*, SP-8007, September.

Nash, W.A. (1957), "Buckling of Initially Imperfect Shells Subject to Torsion," *Journal of Applied Mechanics*, Vol. 24, No. 1.

Osterhof, S.A. and Driver, R.G. (2011), "Performance of the Unified Block Shear Equation for Common Types of Welded Steel Connections," *Engineering Journal*, AISC, Vol. 48, No. 2, pp. 77–92.

Popplewell, W.C. and Coker, E.G. (1895), "Experiments on the Torsional Strength of Solid and Hollow Shafts," *Proceedings of the Institution of Civil Engineers*, Paper No. 2853, pp. 291–298.

Schilling, C.G. (1965), "Buckling Strength of Circular Tubes," *Journal of the Structural Division*, ASCE, Vol. 91, No. ST5.

Schmidt, B.J. and Bartlett, F.M. (2002), "Review of Resistance Factor for Steel: Data Collection," *Canadian Journal of Civil Engineering*, Vol. 29, pp. 98–108.

Schmidt, H. and Wintersetter, T.A. (2004), "Cylindrical Shells under Torsional and Transverse Shear," Chapter 8, *Buckling of Thin Metal Shells*, J.G. Teng and J.M. Rotters, eds., Spon Press.

Schwerin, E. (1924), "Torsional Stability of Thin-Walled Tubes," *Proceedings of the First International Congress for Applied Mechanics*.

Seaburg, P.A. and Carter, C.J. (1997), *Torsional Analysis of Structural Steel Members*, Design Guide 9, AISC, Chicago, Ill.

Seely, F.B. and Putnam, W.J. (1919), "The Relation between the Elastic Strengths of Steel in Tension, Compression and Shear," *Bulletin No. 115*, Engineering Experiment Station, University of Illinois, Urbana-Champaign, Ill.

Seide, P., Weingarten, V.I., and Morgan, E.J. (1960), *The Development of Design Criteria for Elastic Stability of Thin Shell Structures*, Space Technology Laboratories, Inc., December 31.

Sezawa, K. and Kubo, K. (1931), *The Buckling of a Cylindrical Shell under Torsion*, Report No. 76, Vol. VI, No. 10, Aeronautical Research Institute, Tokyo Imperial University, December.

Sherman, D.R. (1975), "Structural Behavior of Tubular Sections," *Proceedings of the International Specialty Conference on Cold-Formed Steel Structures*.

Stang, A.H., Ramberg, W., and Back, G. (1937), "Torsion Tests of Tubes," NACA Technical Report No. 601, National Advisory Committee for Aeronautics.

Sturm, R.G. (1948), "Stability of Thin Cylindrical Shells in Torsion," *Transactions of the American Society of Civil Engineers*, Vol. 113, Paper No. 2345, pp. 681–717.

Timoshenko, S.P. and Gere, J.M. (1961), *Theory of Elastic Stability*, McGraw-Hill.

Wu, C., He, L., Ghafoori, E., and Zhao, X.L. (2018), "Torsional Strengthening of Steel Circular Hollow Sections (CHS) Using CFRP Composites," *Engineering Structures*, Vol. 171.

Yamaki, N. (1974), "Experiments on the Postbuckling Behavior of Circular Cylindrical Shells under Torsion," *Buckling of Structures, Symposium Proceedings*, June 17–21, Springer-Verlag.

Zhang, X. and Han, Q. (2007), "Buckling and Postbuckling Behaviors of Imperfect Cylindrical Shells Subjected to Torsion," *Thin-Walled Structures*, Vol. 45, pp. 1,035–1,043.

Ziemian, R.D. (2010), *Guide to Stability Design Criteria for Metal Structures*, 6th Ed., John Wiley & Sons.

Specimen	D in.	L in.	t in.	E ksi	σ_y ksi	Specimen	D in.	L in.	t in.	E ksi	σ_y ksi
Table A-1. Specimen Details										
Popplewell and Coker (1895)						Donnell (1935) continued					
36	0.500	5.00	0.0935	27,744	34.8	18	5.67	12.0	0.00205	31,300	—[b]
37	0.500	5.00	0.0935	27,744	34.8	19	3.75	12.0	0.00201	31,300	—[b]
38	0.500	5.00	0.0935	27,744	34.8	20	1.88	12.0	0.00201	31,300	—[b]
39	0.501	5.00	0.0920	27,744	34.8	21	1.88	24.0	0.00284	31,300	—[b]
40	0.501	5.00	0.0925	27,744	34.8	22	1.88	30.0	0.00201	31,300	—[b]
Seely and Putnam (1919)						23	0.319	4.53	.00192	31,300	—[b]
L1	2.88	8.25	0.125	29,000[a]	28.4	24	0.319	7.81	.00192	31,300	—[b]
L2	2.63	8.25	0.188	29,000[a]	28.4	25	0.319	12.4	.00192	31,300	—[b]
M1	0.750	3.25	0.125	29,000[a]	33.6	26	0.319	13.1	.00192	31,300	—[b]
M2	0.625	3.25	0.0625	29,000[a]	33.6	27	0.319	15.8	.00190	31,300	—[b]
M3	0.563	3.25	0.0313	29,000[a]	33.6	28	0.319	21.4	.00199	31,300	—[b]
H1	0.625	3.25	0.0625	29,000[a]	45.8	29	0.319	29.5	.00192	31,300	—[b]
Bridget et al. (1934)						30	0.319	53.5	.00192	31,300	—[b]
A	1.88	5.32	.00204	31,400	37.7	Stang et al. (1937)					
C	3.75	5.32	0.00295	30,600	48.6	A1	0.750	19.0	0.0304	29900	84.0
D	1.88	11.32	0.00204	27,060	53.3	A2	0.750	19.0	0.0303	29900	84.0
E	1.88	5.32	0.00295	30,600	48.6	A3	0.751	60.0	0.0302	29900	84.0
F	3.75	1.32	0.00204	31,400	57.7	B1	1.001	19.0	0.0381	28800	89.0
G1	1.88	5.32	0.00395	29,600	36.0	B2	1.001	19.0	0.0380	28800	89.0
G2	1.88	5.32	0.00395	29,600	36.0	B3	1.001	19.0	0.0380	28800	89.0
G3	1.88	5.32	0.00395	29,600	36.0	C1	1.128	19.0	0.0479	29000	93.0
G4	1.88	5.32	0.00395	29,600	36.0	C2	1.127	19.0	0.0480	29000	93.0
Donnell (1935)						C3	1.127	60.0	0.0480	29000	93.0
1	27.0	85.8	0.0115	31,300	—[b]	D1	1.503	19.0	0.0580	29100	99.0
2	5.88	.469	.00193	31,300	—[b]	D2	1.503	19.0	0.0580	29100	99.0
3	5.88	.375	.00193	31,300	—[b]	D3	1.503	19.0	0.0581	29100	99.0
4	5.88	.290	.00193	31,300	—[b]	D4	1.503	19.0	0.0581	29100	99.0
5	5.67	6.00	0.00292	31,300	—[b]	D5	1.503	48.0	0.0581	29100	99.0
6	5.67	6.00	0.00280	31,300	—[b]	E1	2.004	19.0	0.0652	28700	108
7	3.75	6.00	0.00288	31,300	—[b]	E2	2.004	19.0	0.0652	28700	108
8	3.75	6.00	0.00288	31,300	—[b]	E3	2.004	19.0	0.0653	28700	108
9	1.88	6.00	0.00292	31,300	—[b]	E4	2.005	48.0	0.0652	28700	108
10	5.67	6.00	0.00217	31,300	—[b]	F1	1.377	19.0	0.0382	28800	81.0
11	5.67	6.00	0.00217	31,300	—[b]	F2	1.377	19.0	0.0382	28800	81.0
12	3.75	6.00	0.00213	31,300	—[b]	F3	1.385	45.0	0.0381	28800	81.0
13	3.75	6.00	0.00213	31,300	—[b]	G1	1.498	19.0	0.0349	29000	69.2
14	1.88	6.00	0.00205	31,300	—[b]	G2	1.499	19.0	0.0349	29000	69.2
15	5.67	12.0	0.00268	31,300	—[b]	G3	1.498	45.0	0.0349	29000	69.2
16	3.75	12.0	0.00280	31,300	—[b]	H1	1.510	19.0	0.0528	28800	78.6
17	1.88	12.0	0.00280	31,300	—[b]	(Table A-1 continues on the next page)					

Table A-1. Specimen Details (continued)											
Specimen	D in.	L in.	t in.	E ksi	σ_y ksi	Specimen	D in.	L in.	t in.	E ksi	σ_y ksi
Stang et al. (1937) continued						Stang et al. (1937) continued					
I1	1.510	19.0	0.0685	28600	67.7	H2	1.511	19.0	0.0527	28800	78.6
I2	1.510	19.0	0.0687	28600	67.7	S1	1.250	19.0	0.0338	28400	87.8
J1	1.503	19.0	0.0845	28800	82.2	S2	1.251	19.0	0.0338	28400	87.8
J2	1.503	19.0	0.0845	28800	82.2	T1	1.503	19.0	0.0352	28200	93.8
J3	1.503	47.0	0.0845	28800	82.2	T2	1.503	19.0	0.0352	28200	93.8
K1	1.502	19.0	0.0928	28800	110	T3	1.503	60.0	0.0352	28200	93.8
K2	1.503	19.0	0.0925	28800	110	U1	1.505	19.0	0.0501	28800	103.8
L1	1.500	19.0	0.1259	28500	96.0	U2	1.506	19.0	0.0501	28800	103.8
L2	1.499	19.0	0.1258	28500	96.0	U3	1.508	60.0	0.0501	28800	103.8
L3	1.500	45.0	0.1258	28500	96.0	V1	2.500	19.0	0.0341	30200	75.0
M1	1.630	19.0	0.0495	27300	90.5	V2	2.506	19.0	0.0336	30200	75.0
M2	1.631	19.0	0.0495	27300	90.5	V3	2.501	60.0	0.0340	30200	75.0
N1	1.753	19.0	0.0509	27600	96.8	Schmidt and Winterstetter (2004)					
N2	1.752	19.0	0.0509	27600	96.8	1	7.87	7.86	0.0418	29,153	23.9
N3	1.752	45.0	0.0507	27600	96.8	2	7.89	7.85	0.0266	29,443	24.4
O1	1.626	19.0	0.0359	27500	93.0	3	7.89	15.7	0.0420	29,153	23.9
O2	1.625	19.0	0.0358	27500	93.0	4	7.87	15.7	0.0267	29,443	24.4
O3	1.628	60.0	0.0357	27500	93.0	Wu et al. (2018)					
P1	1.751	19.0	0.0356	27600	105	1-1	3.50	14.2	0.120	30,755	58.0
P2	1.752	19.0	0.0354	27600	105	1-2	3.50	14.2	0.120	30,755	58.0
P3	1.751	60.0	0.0354	27600	105	2-1	4.00	16.1	0.119	30,143	44.4
Q1	2.005	19.0	0.0361	27600	99.1	2-2	4.00	16.1	0.119	30,143	44.4
Q2	1.998	60.0	0.0360	27600	99.1	3-1	4.50	18.1	0.143	29,566	45.9
R1	1.124	19.0	0.0316	29000	95.2	3-2	4.50	18.1	0.143	29,566	45.9
R2	1.124	19.0	0.0317	29000	95.2	4-1	4.50	18.1	0.166	29,853	41.2
R3	1.124	60.0	0.0317	29000	95.2	5-1	4.50	18.1	0.201	30,266	53.9

[a] The modulus of elasticity was not measured for these specimens. 29,000 ksi is the nominal value.
[b] The yield stress was not measured for these specimens.

	Experimental		AISC Specification			Proposed		
Specimen	T_e kip-in.	FM	T_c kip-in.	FM	T_e/T_c	T_c kip-in.	FM	T_e/T_c
Table A-2. Experimental Results								
Popplewell and Coker (1895)								
36	0.475[a]	Y	0.507	Y	0.937	0.507	Y	0.937
37	0.425[a]	Y	0.507	Y	0.838	0.507	Y	0.838
38	0.425[a]	Y	0.507	Y	0.838	0.507	Y	0.838
39	0.425[a]	Y	0.505	Y	0.842	0.505	Y	0.842
40	0.425[a]	Y	0.507	Y	0.839	0.507	Y	0.839
Seely and Putnam (1919)								
L1	21.2[a]	Y	25.3	Y	0.839	25.3	Y	0.839
L2	28.9[a]	Y	29.8	Y	0.968	29.8	Y	0.968
M1	1.61[a]	Y	1.55	Y	1.042	1.55	Y	1.042
M2	0.662[a]	Y	0.626	Y	1.057	0.626	Y	1.057
M3	0.273[a]	Y	0.279	Y	0.977	0.279	Y	0.977
H1	0.836[a]	Y	0.854	Y	0.979	0.854	Y	0.979
Bridget et al. (1934)								
A	0.0550	B	0.0511	I	1.08	0.0353	I	1.56
C	0.217	B	0.271	I	0.801	0.187	I	1.16
D	0.0360	B	0.0302	I	1.19	0.0209	I	1.73
E	0.106	B	0.114	I	0.929	0.0789	I	1.34
F	0.160	B	0.243	I	0.657	0.168	I	0.951
G1	0.178	B	0.213	I	0.837	0.147	I	1.21
G2	0.196	B	0.213	I	0.921	0.147	I	1.33
G3	0.186	B	0.213	I	0.874	0.147	I	1.27
G4	0.184	B	0.213	I	0.865	0.147	I	1.25
Donnell (1935)								
1	12.8	B	16.1	I	0.797	11.1	I	1.15
2	0.960	B	0.631	I	1.52	0.436	I	2.20
3	1.02	B	0.705	I	1.45	0.488	I	2.09
4	1.40	B	0.802	I	1.75	0.554	I	2.53
5	0.286	B	0.428	I	0.669	0.296	I	0.968
6	0.268	B	0.389	I	0.689	0.269	I	1.00
7	0.202	B	0.247	I	0.817	0.171	I	1.18
8	0.218	B	0.247	I	0.882	0.171	I	1.28
9	0.096	B	0.107	I	0.894	0.0742	I	1.29
10	0.162	B	0.219	I	0.738	0.152	I	1.07
11	0.146	B	0.219	I	0.666	0.152	I	0.963
12	0.0840	B	0.125	I	0.670	0.0867	I	0.969
13	0.106	B	0.125	I	0.845	0.0867	I	1.22
14	0.0460	B	0.0485	I	0.949	0.0335	I	1.37
15	0.206	B	0.249	I	0.826	0.172	I	1.20

(Table A-2 continues on the next page)

	Experimental		AISC *Specification*			Proposed		
Specimen	T_e kip-in.	FM	T_c kip-in.	FM	T_e/T_c	T_c kip-in.	FM	T_e/T_c
Table A-2. Experimental Results (continued)								
Donnell (1935) continued								
16	0.128	B	0.164	I	0.780	0.113	I	1.13
17	0.0640	B	0.069	I	0.926	0.0478	I	1.34
18	0.0900	B	0.136	I	0.659	0.0943	I	0.954
19	0.0600	B	0.0778	I	0.771	0.0538	I	1.12
20	0.032	B	0.0328	I	0.975	0.0227	I	1.41
21	0.048	B	0.0504	I	0.952	0.0349	I	1.38
22	0.0200	B	0.0207	I	0.964	0.0143	I	1.39
23	0.00520	B	0.00364	I	1.43	0.00359	I	1.45
24	0.00339	B	0.00364	I	0.932	0.00273	I	1.24
25	0.00381	B	0.00314	I	1.21	0.00266	L	1.43
26	0.00341	B	0.00305	I	1.12	0.00266	L	1.28
27	0.00319	B	0.00272	I	1.17	0.00259	L	1.23
28	0.00301	B	0.00291	L	1.04	0.00291	L	1.04
29	0.00327	B	0.00266	L	1.23	0.00266	L	1.23
30	0.00320	B	0.00266	L	1.20	0.00266	L	1.20
Stang et al. (1937)								
A1	1.25	B	1.25	Y	1.00	1.25	Y	1.00
A2	1.24	B	1.24	Y	1.00	1.24	Y	1.00
A3	1.26	B	1.24	Y	1.01	1.24	Y	1.01
B1	3.16	B	2.96	Y	1.07	2.96	Y	1.07
B2	3.17	B	2.96	Y	1.07	2.96	Y	1.07
B3	3.19	B	2.96	Y	1.08	2.96	Y	1.08
C1	4.95	B	4.90	Y	1.01	4.90	Y	1.01
C2	4.98	B	4.90	Y	1.02	4.90	Y	1.02
C3	5.07	B	4.90	Y	1.03	4.90	Y	1.03
D1	11.7	B	11.3	Y	1.04	11.3	Y	1.04
D2	11.8	B	11.3	Y	1.04	11.3	Y	1.04
D3	11.7	B	11.3	Y	1.03	11.3	Y	1.03
D4	11.6	B	11.3	Y	1.02	11.3	Y	1.02
D5	11.4	B	11.3	Y	1.01	11.3	Y	1.01
E1	23.4	B	24.9	Y	0.940	24.9	Y	0.940
E2	22.8	B	24.9	Y	0.912	24.9	Y	0.912
E3	23.2	B	25.0	Y	0.931	25.0	Y	0.931
E4	23.1	B	25.0	Y	0.924	25.0	Y	0.924
F1	5.74	B	5.23	Y	1.10	5.23	Y	1.10
F2	5.73	B	5.23	Y	1.10	5.23	Y	1.10
F3	5.75	B	5.28	Y	1.09	5.28	Y	1.09
G1	5.40	B	4.87	Y	1.11	4.87	Y	1.11
Table A-2 continues on the next page								

Table A-2. Experimental Results (continued)								
	Experimental		AISC *Specification*			Proposed		
Specimen	T_e kip-in.	FM	T_c kip-in.	FM	T_e/T_c	T_c kip-in.	FM	T_e/T_c
Stang et al. (1937) continued								
G2	5.39	B	4.88	Y	1.11	4.88	Y	1.11
G3	5.54	B	4.87	Y	1.14	4.87	Y	1.14
H1	8.89	B	8.31	Y	1.07	8.31	Y	1.07
H2	8.77	B	8.30	Y	1.06	8.30	Y	1.06
I1	12.1	B	9.08	Y	1.34	9.08	Y	1.34
I2	11.7	B	9.11	Y	1.29	9.11	Y	1.29
J1	17.5	B	13.2	Y	1.33	13.2	Y	1.33
J2	17.5	B	13.2	Y	1.33	13.2	Y	1.33
J3	17.4	B	13.2	Y	1.32	13.2	Y	1.32
K1	19.9	B	19.1	Y	1.04	19.1	Y	1.04
K2	19.9	B	19.1	Y	1.04	19.1	Y	1.04
L1	23.5	B	21.5	Y	1.09	21.5	Y	1.09
L2	22.7	B	21.5	Y	1.06	21.5	Y	1.06
L3	22.2	B	21.5	Y	1.03	21.5	Y	1.03
M1	10.8	B	10.5	Y	1.03	10.5	Y	1.03
M2	11.2	B	10.6	Y	1.06	10.6	Y	1.06
N1	14.5	B	13.5	Y	1.08	13.5	Y	1.08
N2	14.3	B	13.4	Y	1.06	13.4	Y	1.06
N3	14.2	B	13.4	Y	1.06	13.4	Y	1.06
O1	7.78	B	7.96	Y	0.978	7.96	Y	0.978
O2	7.87	B	7.92	Y	0.993	7.92	Y	0.993
O3	7.96	B	7.62	L	1.05	7.62	L	1.05
P1	9.71	B	10.4	Y	0.937	9.00	I	1.08
P2	9.49	B	10.3	Y	0.919	8.89	I	1.07
P3	9.17	B	7.79	L	1.18	7.79	L	1.18
Q1	12.4	B	13.1	Y	0.949	11.0	I	1.12
Q2	11.6	B	8.90	I	1.30	8.72	L	1.33
R1	3.38	B	3.38	Y	1.00	3.38	Y	1.00
R2	3.50	B	3.39	Y	1.03	3.39	Y	1.03
R3	3.62	B	3.39	Y	1.07	3.39	Y	1.07
S1	4.16	B	4.14	Y	1.01	4.14	Y	1.01
S2	4.15	B	4.14	Y	1.00	4.14	Y	1.00
T1	6.58	B	6.70	Y	0.981	6.70	Y	0.981
T2	6.54	B	6.70	Y	0.975	6.70	Y	0.975
T3	6.30	B	6.70	Y	0.940	6.70	Y	0.940
U1	10.3	B	10.4	Y	0.991	10.4	Y	0.991
U2	10.3	B	10.4	Y	0.989	10.4	Y	0.989
U3	10.4	B	10.4	Y	0.994	10.4	Y	0.994
(Table A-2 continues on the next page)								

	Experimental		AISC *Specification*			Proposed		
	T_e kip-in.	FM	T_c kip-in.	FM	T_e/T_c	T_c kip-in.	FM	T_e/T_c
Specimen								
Stang et al. (1937) continued								
V1	13.5	B	14.7	Y	0.918	14.1	I	0.952
V2	13.1	B	14.5	Y	0.900	13.7	I	0.952
V3	9.59	B	11.4	I	0.838	9.34	L	1.03
Schmidt and Winterstetter (2004)								
1	59.0	B	57.8	Y	1.02	57.8	Y	1.02
2	43.3	B	37.8	Y	1.15	37.8	Y	1.15
3	59.0	B	58.4	Y	1.01	58.4	Y	1.01
4	41.5	B	37.7	Y	1.10	37.4	I	1.11
Wu et al. (2018)								
1-1	66.4[a]	Y	74.7	Y	0.888	74.7	Y	0.888
1-2	66.4[a]	Y	74.7	Y	0.888	74.7	Y	0.888
2-1	66.4[a]	Y	74.9	Y	0.886	74.9	Y	0.886
2-2	66.4[a]	Y	74.9	Y	0.886	74.9	Y	0.886
3-1	106[a]	Y	117	Y	0.904	117	Y	0.904
3-2	106[a]	Y	117	Y	0.904	117	Y	0.904
4-1	124[a]	Y	121	Y	1.02	121	Y	1.02
5-1	204[a]	Y	189	Y	1.08	189	Y	1.08

Table title: **Table A-2. Experimental Results (continued)**

[a] For these specimens, the ultimate experimental torsion resulted in large inelastic rotation angles. The proportional limit on the torsion-rotation curve was used for the experimental torsion.

T_c = calculated torsional moment, kip-in.

T_e = experimental torsional moment, kip-in.

FM: Failure mode

B: Buckling

I: Buckling of an intermediate-length member

L: Buckling of a long member

Y: Yield